

Triplet exciton energy transfer in polyfluorene doped with heavy metal complexes studied using photoluminescence and photoinduced absorption

H. H. Liao,^{1,2} H. F. Meng,^{1,*} S. F. Horng,² W. S. Lee,¹ J. M. Yang,² C. C. Liu,² J. T. Shy,³ F. C. Chen,⁴ and C. S. Hsu⁵

¹*Institute of Physics, National Chiao Tung University, Hsinchu 300, Taiwan, Republic of China*

²*Department of Electric Engineering, National Tsing Hua University, Hsinchu 300, Taiwan, Republic of China*

³*Department of Physics, National Tsing Hua University, Hsinchu 300, Taiwan, Republic of China*

⁴*Institute of Display, National Chiao Tung University, Hsinchu 300, Taiwan, Republic of China*

⁵*Department of Applied Chemistry, National Chiao Tung University, Hsinchu 300, Taiwan, Republic of China*

(Received 12 April 2006; revised manuscript received 24 October 2006; published 15 December 2006)

Modulated photoinduced absorption and photoluminescence are used to study triplet-to-triplet Dexter energy transfer in Ir-complexes/polyfluorene blend systems. There is no Dexter energy transfer for red iridium (III)bis[2-(9,9-dibutylfluorenyl)-1-isoquinoline(acetylacetonate)] (DFIr) and red iridium (III) bis([2-(2-benzo-thienyl)pyridinatoN,C3] acetyl-acetonate) (BtpIr) dopants. Although green iridium(III)tris[2-(4-tolyl)pyridinato-N,C2] [Ir(mppy)₃] has no triplet confinement in polyfluorene host, it has clear evidence for Dexter energy transfer. Aggregation and dopant lifetime are shown to significantly affect the energy transfer. The presence of Dexter transfer implies the possibility to harvest triplet excitons of polyfluorene in polymer light-emitting diodes even without carrier trapping and triplet exciton confinement.

DOI: [10.1103/PhysRevB.74.245211](https://doi.org/10.1103/PhysRevB.74.245211)

PACS number(s): 71.35.-y

I. INTRODUCTION

The formation and decay of spin-triplet excitons in polymer light-emitting diodes (PLED's) are important and hotly debated subjects, partially because they determine the theoretical limit of the quantum efficiency for both fluorescent and phosphorescent PLED's.¹ Among all the processes involved in luminescence, triplet-to-triplet energy transfer is probably the most elusive and least understood. Because only spin-singlet excitons of conjugated polymers emit light, the triplet-to-singlet branching ratio γ determines the quantum efficiency of fluorescent PLED's.¹⁻³ In our previous study using infrared-induced absorption⁴ it is found that γ is a constant independent of electric field and temperature, suggesting that the exciton formation process is spin independent. This is consistent with a recent magnetic resonance experiment.⁵ It is therefore expected that the branching ratio for the nonemissive triplet excitons in PLED is no different from small-molecule light-emitting diodes (OLED's)—i.e., $\gamma=3$ for both cases.⁶ These results imply that to harvest the 75% nonemissive triplet excitons in PLED's is essential for achieving highly efficient PLED's, just like the well-established case of OLED's. A full understanding of the triplet exciton in polymer is therefore highly desired.

The most promising way to harvest the triplet energy is to take the same strategy as OLED's and introduce heavy-metal triplet emitters into the polymer to make phosphorescent PLED's (PhPLED's).⁷⁻⁹ Indeed by employing triplet emitters the efficiency of PLED's is significantly improved¹⁰⁻¹² but is still far below OLED's. So far the reason for this difference is not clear and the basic physics of PhPLED's is unknown. In the early period of phosphorescent small-molecule OLED's (PhOLED's), triplet emitters are considered to harvest triplet excitons of the host by triplet-to-triplet Dexter energy transfer.^{7,8,13,14} Afterward, however, the high efficiency of PhOLED's is reported to be caused by carrier trapping^{9,10,15,16} which is a sequential process of electron and

hole capture by the triplet emitters followed by direct recombination. It turns out that Dexter energy transfer and trapping mechanisms dominate in different host/guest PhOLED systems.¹⁷ As for PhPLED's, previous studies show that there is no Dexter energy transfer in main-chain conjugated polymers doped by a phosphor emitter,¹⁸⁻²⁰ in particular the common conjugated polymer host polyfluorene doped by Ir-complex phosphors. Dexter energy transfer is found only in side-chain conjugation polymers poly(vinylcarbazole) (PVK) at extremely low temperature. It is therefore an outstanding question whether the triplet excitons of polyfluorene can be harvested by triplet emitters through Dexter energy transfer to achieve highly efficient PhPLED's or high efficiency can only be realized through trapping mechanisms by triplet emitters like the situation of PhOLED's. In order to answer this question, in this work we use two polyfluorenes and three Ir complexes to study Dexter energy transfer in phosphor-doped conjugated polymer systems. Using our infrared-induced absorption setup,⁴ we are able to monitor the behaviors of the three primary photoexcitations in the polymer/phosphor system, i.e., singlet exciton of the host polymer, triplet exciton of the host polymer, and triplet exciton of the phosphor. By comparing the decay dynamics of the polymer triplet exciton and phosphor triplet exciton, we observed Dexter energy transfer for a green Ir complex but not red complexes despite the lack of triplet exciton confinement in the green complex. The film morphology study shows that the blend with green Ir complex is more uniform than others. The triplet exciton lifetime is also shown to be critical to decide whether the transfer occurs or not.

II. EXPERIMENT

The triplet exciton is detected by photoinduced absorption (PA).⁴ Figure 1 shows the experimental setup for the PA spectroscopy. A 20-mW, 405-nm pump laser (Power Technology) is modulated by a function generator (HP 33120A)

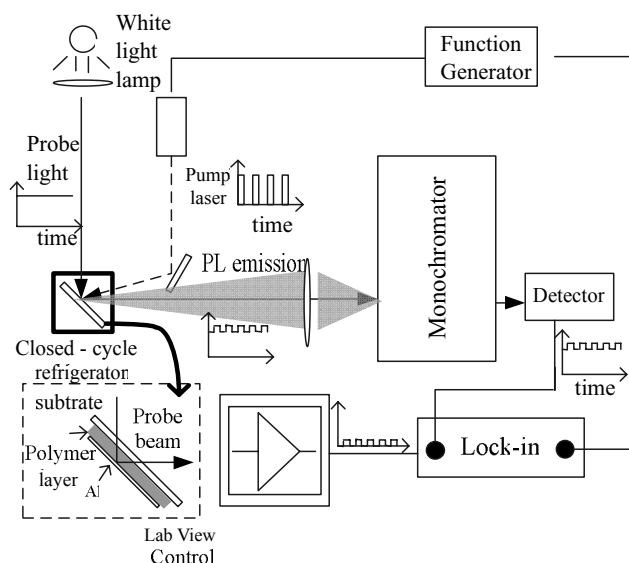


FIG. 1. The setup of PA and quadrature-phase channel PL experiment. The inset is the sample structure and the optical path.

with a square-wave form, and the laser beam is focused on the sample and generates the modulated singlet exciton density. The sample is placed in a low-temperature closed-cycle refrigerator (Janis CCS-150, 10–300 K). Some singlet excitons decay to the ground state, and others become triplet excitons through intersystem crossing (ISC) process. The triplet exciton generation is also modulated due to the modulation of singlet exciton density. Although it is not possible to detect the triplet exciton by its radiative decay due to spin selection rule, we can detect them by its spin-allowed higher-level absorption. A continued-wave (CW) white light probe beam generated by a 250-W quartz-tungsten-halogen lamp is focused on the same spot of the sample as the probe. The probe beam goes through the glass substrate, then the polymer film, and is reflected by a Al layer coated on the polymer film. The optical path of the probe beam is shown in the inset of Fig. 1. The reflected probe beam contains two parts including a modulated component caused by the triplet-exciton higher-level absorption and a remnant CW component. The reflected beam is collected into a monochromator (CVI DK240, with a 700-nm high-pass filter) and detected by a Si detector (New Focus 2001, with 10^3 gain), which is connected to a lock-in amplifier (SRS 830) whose reference channel is connected to the synchronous port of the function generator. The detector receives a small modulated ac and a dc signal. The dc part is removed by the dc filter of the lock-in amplifier, and only the ac signal with the same frequency of the function generator will be extracted and displayed in the in-phase and quadrature-phase channels. All the instruments and the data are controlled and recorded by the Labview program through IEEE-488 interface. When the pump modulation frequency is lower than $1/(2\pi\tau_T)$, where τ_T is host triplet exciton lifetime, the signal will only appear in the in-phase channel of the lock-in amplifier. When the modulation frequency is higher than $1/(2\pi\tau_T)$, the signal in the in-phase channel starts to decay and the signal starts to appear in the quadrature-phase channel of the amplifier.

When the modulation is even faster so that the triplet excitons do not respond to the modulation, the quadrature-phase channel will decay eventually.²¹ Analyzing the phase relation at different frequencies enables one to distinguish a slow signal (with long lifetime, in the quadrature-phase channel) superimposed on a fast signal (with short lifetime, in the in-phase channel).^{22,24} Theoretically frequency domain measurement should give equivalent information as the time domain measurement. Since the relevant time scales in this problem are the triplet exciton lifetime and the Dexter transfer over milliseconds,²⁶ it is more convenient to work in the frequency domain up to only kHz. It is also easy to separate the fast Ir intrinsic emission from the slow emission from Dexter transfer in the polymer/phosphor blended system by the different frequency response. Two polyfluorenes are used: poly(9,9-dioctylfluorenyl-2,7-diyl) end capped with dimethylphenyl (PFO-DMP) and poly[9,9-di-(2-ethylhexyl)fluorenyl-2,7-diyl] end capped with N,N-bis(4-methylphenyl)-4-aniline (PF-MPA). Three Ir complexes are used: iridium(III)tris[2-(4-tolyl)pyridinato-N, C2] [Ir(mppy)₃], iridium (III) bis[2-(9,9-dibutylfluorenyl)-1-isoquinoline(acetylacetonate)] (DFIr), and iridium (III) bis[2-(2-benzo-thienyl)pyridinatoN, C3](acetyl-acetonate) (BtpIr). These materials are all purchased from American Dye Source.

III. MODULATION SPECTRA

Figure 2 shows the relevant transitions. The Ir triplet exciton can be formed by either the Förster or Dexter energy transfer route. The former has a fast response to modulation because of the sub-nanosecond lifetime of host singlet exciton. The latter has long transient because the host triplet exciton lifetime τ_T is in the ms range at low temperature, which is far longer than temperature-independent iridium lifetime τ_{Ir} in the μ s range. Therefore, if both Förster energy transfer and Dexter energy transfer occur, the emission of Ir will have a fast component in the μ s (τ_{Ir}) time scale and a delayed component in the ms (τ_T) time scale. We use a lock-in amplifier to monitor the delayed photoluminescence (PL) at the modulation frequency f such that $1/2\pi\tau_T < f < 1/2\pi\tau_{Ir}$. The fast Ir emission signals from Förster energy transfer ($f < 1/2\pi\tau_T$) will always appear in the in-phase channel of the amplifier and the delayed Ir emission from Dexter energy transfer ($f < 1/2\pi\tau_{Ir}$) will appear in the quadrature-phase channel. By comparing the dynamics of the host triplet exciton detected by PA and guest triplet exciton detected by PL, we are able to unambiguously decide if Dexter energy transfer happens in Ir-complex-doped polyfluorene.

Ir(mppy)₃ and DFIr are dissolved in xylene and BtpIr in tetrahydrofuran (THF). We try four doping concentrations (0%, 5%, 10%, 20%) and compared these solutions. The highest concentrations in which Ir complexes can be well dissolved without any precipitation are 20%, 10%, and 5% for Ir(mppy)₃, DFIr, and BtpIr, respectively. The solution is then spin-coated to form a 100-nm-thick film on a precleaned glass substrate. A 1000-Å Al layer is evaporated on the polymer film as the reflection coating. The PA frequency depen-

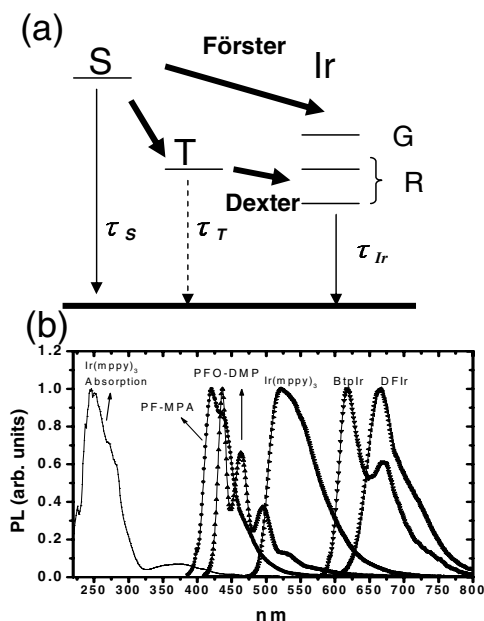


FIG. 2. (a) shows the relative exciton energies of the materials. τ_S and τ_T are host singlet and triplet exciton lifetimes, respectively. Förster energy transfer is from host singlet excitons to Ir singlet excitons and then to its triplet excitons. Dexter energy transfer is from host triplet excitons to Ir triplet excitons. The labels *S* and *T* are for first singlet excited state and first triplet excited state. The energy levels of Ir represent the energy levels of Ir-complex triplet excitons. (b) shows the absorption and emission spectrum of the materials.

dence of the red DFir- or red BtpIr-doped and intrinsic PFO-DMP films at 24 K are shown in Fig. 3(a). All Ir dopants are compared at the same concentration of 10% despite some precipitation for BtpIr. The effect of concentration will be discussed below. There is no difference between two red Ir-doped and intrinsic PFO-DMP triplet excitons, indicating that the host triplet exciton lifetime τ_T is not influenced by DFir and BtpIr. From Fig. 3(a) and the relation $\tau = 1/(2\pi f)$ the PFO-DMP triplet exciton lifetime is approximately 15 ms (at $f=10$ Hz).²¹ Figures 3(b) and 3(c) are the normalized quadrature-phase channel PL spectra of PFO-DMP doped with BtpIr and DFir, respectively. As described above, if the modulation frequency exceeds $1/(2\pi\tau_T)$, the delayed Ir triplet excitons from Dexter energy transfer would appear in the quadrature-phase channel. Although the delayed red PL signals do appear in the quadrature-phase channel as shown in Figs. 3(b) and 3(c), it is not due to Dexter energy transfer because the delayed signal appears in the blue host singlet exciton simultaneously. The spectra at different modulation frequencies are all the same after normalization, implying that the red and blue peaks are delayed by the same mechanism. We attribute this to the weak delayed fluorescence caused by the triplet-triplet annihilation.¹⁷ Through Förster energy transfer the delayed singlet excitons are transferred to Ir to form the delayed Ir emissions. There is no Dexter energy transfer in PFO-DMP doped by either BtpIr or DFir.

The PA frequency dependence of green Ir(mppy)₃ doped PFO-DMP is also shown in Fig. 3(a). The striking difference from the red Ir complexes BtpIr and DFir is that Ir(mppy)₃

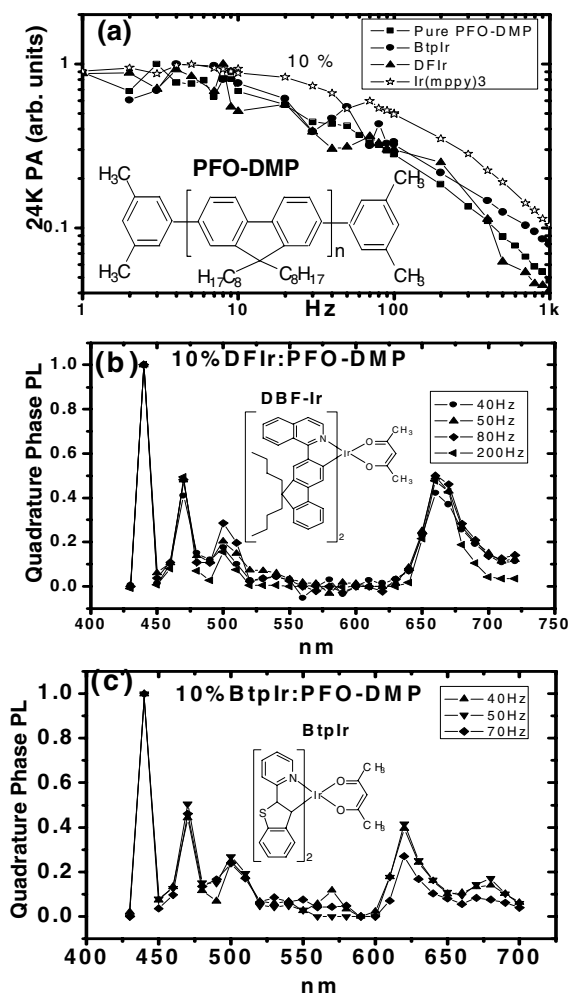


FIG. 3. (a) is the PA frequency dependence of pure PFO-DMP and Ir-complex-doped PFO-DMP films. The inset is the structure of PFO-DMP. (b) is the quadrature-phase channel PL spectrum of 10% DFir:PFO-DMP film. The inset is the structure of DFir. (c) is the quadrature-phase channel PL spectrum of 10% BtpIr:PFO-DMP film. The inset is the structure of BtpIr.

significantly affects the modulation response of the host triplet exciton and the host triplet lifetime is decreased by 2 times in magnitude to 8 ms (~ 20 Hz). This indicates that there is a new channel for the decay of the host triplet exciton. In order to decide if this additional channel is Dexter energy transfer, the host triplet and Ir triplet excitons are monitored by PA and quadrature-phase channel PL measurements, respectively. It is seen in Fig. 4(a) that the PA in-phase channel signal starts to decrease and the PA quadrature-phase channel begins to rise as the frequency is larger than the host triplet exciton lifetime τ_T .

The key feature is that the delayed PA signal directly translates to the quadrature-phase channel as a slow component of green Ir-complex PL. In fact the quadrature-phase channel of Ir PL monitored at its emission peak at 535 nm has an identical frequency response to the PA quadrature-phase channel signals. This correlation between PA and PL suggests that the delayed emission of Ir(mppy)₃ is due to the Dexter route from the host triplet excitons. The normalized quadrature-phase channel PL spectra at different frequencies

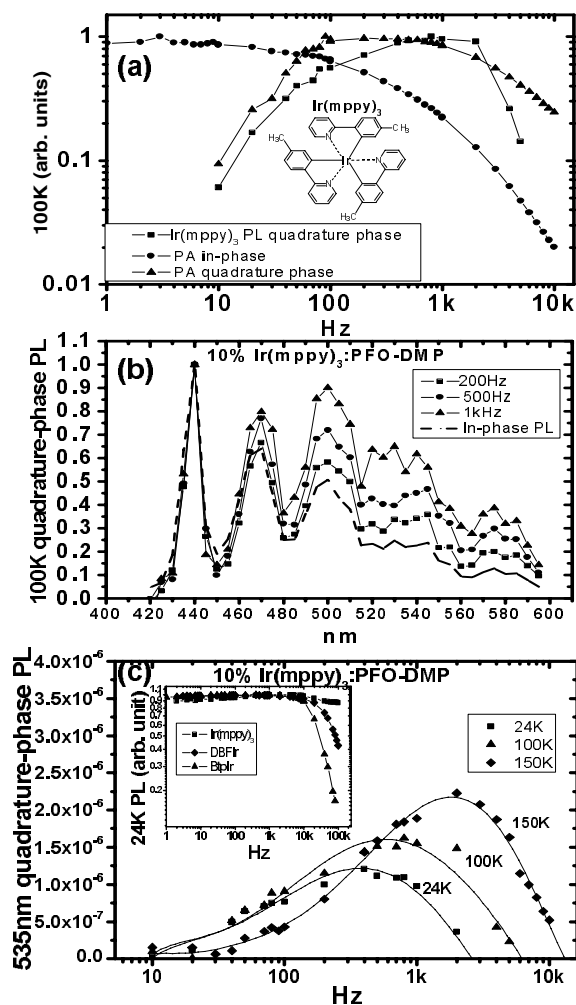


FIG. 4. (a) shows the in-phase channel PA, quadrature-phase channel PA and quadrature-phase channel PL frequency dependences of 10% Ir(mppy)₃:PFO-DMP films at 100 K. The inset is the structure of Ir(mppy)₃. (b) is the quadrature-phase channel PL spectra normalized at 439 nm at different modulation frequency and an in-phase PL spectrum. (c) is the Ir(mppy)₃ emission peak quadrature-phase PL frequency dependences at three temperatures. The inset is the in-phase PL frequency dependences of three Ir complexes.

and the in-phase channel PL spectrum of the Ir(mppy)₃:PFO-DMP system are shown in Fig. 4(b). Although quadrature-phase channel PL spectra also show the delayed fluorescence coming from the triplet-triplet annihilation as in red Ir complexes, the magnitude of the green Ir(mppy)₃ emission is strongly frequency dependent, contrary to the previous cases of BtpIr and DFIr. Indeed this green component is prominent only when the frequency is around $1/2\pi\tau_T$. This delayed extra Ir emission cannot come from the delayed fluorescence through Förster energy transfer because of the apparent difference in modulation responses at a frequency far smaller than the inverse of both of their intrinsic lifetimes. Dexter energy transfer from the host triplet to guest triplet is the only possibility to explain these results.

Further proof comes from the temperature dependence. Since the delayed Ir emission comes from the host triplet

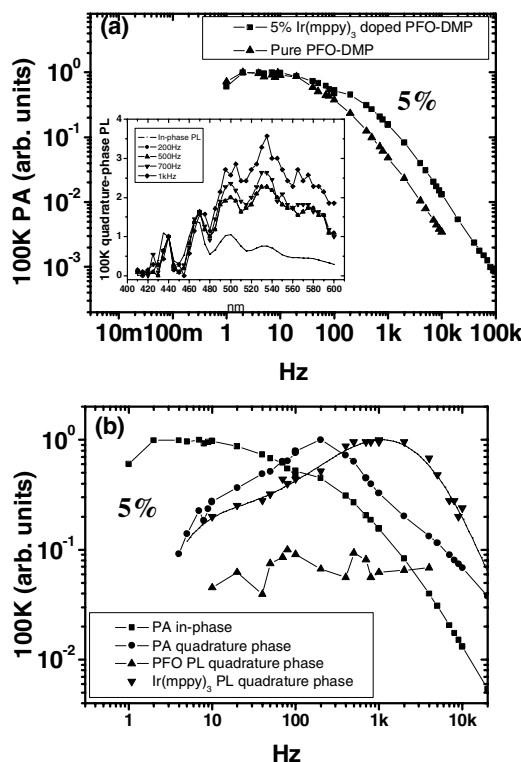


FIG. 5. (a) is the normalized PA at 100 K for 5% Ir(mppy)₃-doped PFO-DMP and pure PFO-DMP. Inset is a 5% Ir(mppy)₃-doped PFO-DMP quadrature-phase channel PL spectrum at different frequency and in-phase channel PL spectrum. (b) shows the Ir(mppy)₃ in-phase channel PA, Ir(mppy)₃ quadrature-phase channel PA, PFO-DMP PL quadrature-phase channel PL, and Ir(mppy)₃ quadrature-phase channel PL frequency dependences. The PFO-DMP PL quadrature-phase channel PL is almost frequency independent.

excitons, it must have a strong temperature dependence as the host triplet exciton lifetime decreases rapidly with rising temperature.⁴ Figure 4(c) shows the delayed PL of Ir(mppy)₃ at three temperatures. It is obvious that when the temperature is increased the maximum is shifted to higher frequency, indicating that the delay is shortened at higher temperature. This provides strong evidence that the Ir emission is derived from the host triplet exciton. The uncertainty in the existence of triplet-to-triplet Dexter energy transfer in PLED doped with phosphor is therefore settled. Another host polyfluorene polymer PF-MPA is doped by Ir(mppy)₃. It is found that all general features are the same as PFO-DMP doped by Ir(mppy)₃. The Dexter energy transfer to Ir(mppy)₃ is therefore expected to be a general behavior for polyfluorene.

IV. MORPHOLOGY AND CONCENTRATION EFFECTS

In Fig. 5(a), PFO-DMP doped by 5% Ir(mppy)₃ is also measured in order to study the concentration effects. The PFO-DMP triplet exciton lifetime is reduced from 1.8 ms to 0.5 ms by Ir(mppy)₃ doping at 100 K. Figure 5(b) shows PA in-phase, PA quadrature-phase, and Ir(mppy)₃ PL

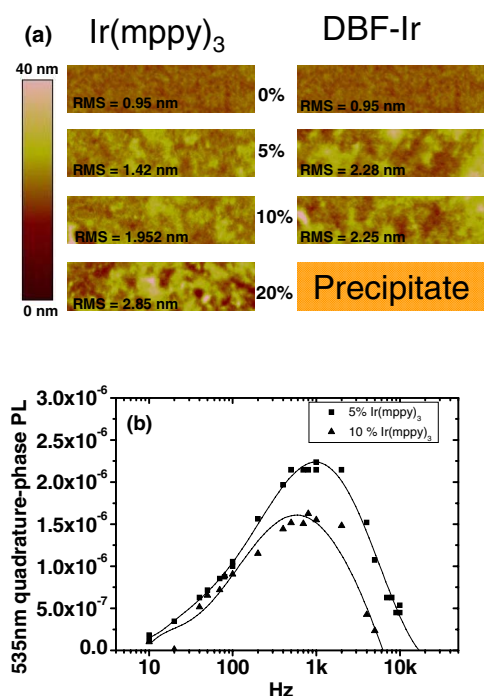


FIG. 6. (Color) (a) shows the AFM images for Ir(mppy)₃ and DFIr with four different doping concentrations. (b) is the un-normalized Ir(mppy)₃ quadrature-phase channel PL intensity at emission peak 535 nm. The 5% Ir(mppy)₃-doped PFO-DMP film has a better morphology than 10% Ir(mppy)₃, so that Dexter energy transfer is more efficient for 5% doping.

quadrature-phase frequency modulations, which are all similar to 10% results and indicate that Dexter energy transfer exists for 5% as well. Atomic-force microscope (AFM) is used to characterize the concentration dependence of the morphology. AFM images of two dopants with four different doping concentrations are shown in Fig. 6(a). BtpIr results are not shown here because they have precipitations when the concentration is over 5% and the optical microscope image shows the film is very rough, indicating that the aggregation of BtpIr in PFO-DMP is so serious that the host/guest average distance is not short enough to make Dexter energy transfer happen. For Ir(mppy)₃, the root-mean-square (rms) roughness increases with doping concentration and does not exceed 2 nm before 10%. When 5% DFIr is doped into PFO-DMP, the roughness immediately exceeds 2 nm, but the roughness is not changed when the concentration is 10%. This means that the DFIr morphology is less uniform than Ir(mppy)₃, and it might be the reason why Dexter energy transfer cannot be observed in DFIr doped PFO-DMP systems. Twenty percent of the DFIr-doped PFO-DMP solution has precipitation, so the AFM image is not shown. Figure 6(b) shows the un-normalized Ir(mppy)₃ quadrature-phase PL intensity for 5% and 10% doping concentrations. Interestingly 5% has higher quadrature-phase PL intensity than 10%, implying that Dexter energy transfer from the PFO-DMP triplet state to Ir(mppy)₃ is more efficient at 5% doping. Since the morphology of 5% is more uniform than 10% doping as shown in Fig. 6(a), Dexter energy transfer efficiency is significantly correlated to the film morphology.

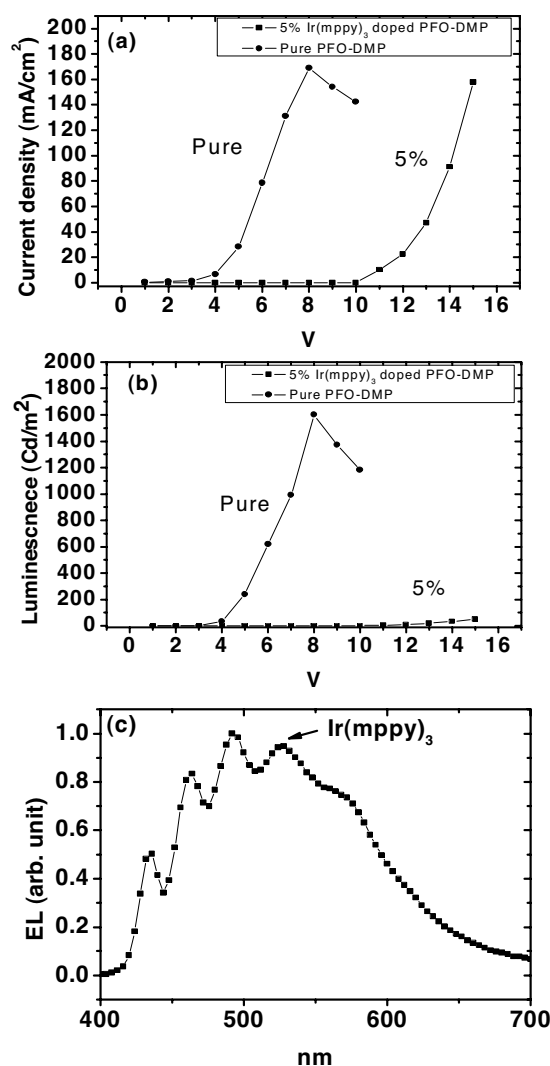


FIG. 7. EL device characteristics for 5% Ir(mppy)₃-doped PFO-DMP and pure PFO-DMP. (a) is current density versus voltage. (b) is luminescence versus voltage. (c) is the 5% Ir(mppy)₃-doped PFO-DMP EL spectrum.

V. ELECTROLUMINESCENCE

Figure 7 shows the device electroluminescence (EL) characteristics of 5% Ir(mppy)₃ doped PFO-DMP and pure PFO-DMP. The device structure is ITO/PEDOT:PSS/polymer (1000 Å)/CsF(10 Å)/Al (1000 Å). PEDOT:PSS is the hole injection polymer poly(3,4-ethylenedioxythiophene) doped with polystyrene sulphonated acid. The device turn-on voltage is increased enormously from 3 V to 10 V, apparently due to Ir(mppy)₃ carrier trapping induced by Ir(mppy)₃. The device efficiency is very poor, indicating huge imbalance of electron and hole by the trapping. Although we prove that Dexter energy transfer exists in polyfluorene doped by Ir complex under optical excitation, this blend system is often dominated by the trapping mechanism in an organic phosphorescent EL device—for example, 4,4'-N,N'-dicarbazole-biphenyl (CBP) doped by *fac* tris(2-phenylpyridine)iridium [Ir(mppy)₃].⁶ However, recently it is demonstrated that the Ir(mppy)₃:CBP system can still use

Dexter energy transfer to achieve high EL efficiency with proper multilayer structures.²⁷ These works indicate that Ir-doped polyfluorene also has the possibility to use Dexter energy transfer to achieve high EL efficiency if the morphology problems are overcome and a proper multilayer structure can be fabricated.²⁸

VI. DISCUSSIONS AND RATE EQUATIONS

The interesting remaining question is what causes the different behaviors of green Ir(mppy)₃ and the two red Ir complexes. The triplet exciton levels of the red-emitting DFIr and BtpIr are smaller than the PFO-DMP triplet exciton level as shown in Fig. 2(a). Despite the good triplet exciton confinement,²³ there is surprisingly no Dexter energy transfer in these two cases. On the other hand, there is no (or poor) triplet exciton confinement for Ir(mppy)₃. Nevertheless, Dexter energy transfer does exist. This illustrates that the triplet exciton confinement is not the main condition for Dexter energy transfer in Ir-doped polyfluorene systems as previously believed.²³ The main differences between two red Ir complexes and Ir(mppy)₃ are the aggregation and decay lifetime. BtpIr has serious aggregation even in good solvent THF. Although DFIr has fluorene ligands and good solubility,¹⁵ the morphology is not as uniform as Ir(mppy)₃ in polyfluorene. So Dexter energy transfer can only be observed in Ir(mppy)₃-doped systems, with a uniform distribution of dopants. The average distance between the host exciton and the dopant is therefore much smaller for a given doping concentration. The second important factor is the fast triplet exciton lifetime for Ir(mppy)₃. From in-phase PL shown in the inset of Fig. 4(c), the lifetimes of BtpIr and DFIr are 16 μs (at 10 kHz) and 5 μs (at 30 kHz),²⁵ respectively. On the other hand, the PL in-phase channel signals do not have a significant drop in our frequency range (from 1 Hz to 100 kHz), indicating that Ir(mppy)₃ triplet lifetime is far below 1 μs.¹⁴ With fast decay at the dopant, the triplet exciton can hardly come back to the host once transferred to the dopant. The dopant therefore becomes an efficient drain of the triplet energy than the host itself.

The general behaviors of Dexter energy transfer can be quantitatively modeled by the rate equations. Consider first the situation that the guest triplet exciton energy is higher than the host triplet exciton, presumably the case for the green Ir complex. Let the energy difference be Δ. Assume the host triplet exciton density is n_T per host monomer and the guest molecule density is n_g per host monomer. n_T and n_g are both dimensionless and n_g is always smaller than 1. f is the probability that the guest molecule is in its triplet excited state—i.e., that there is one triplet exciton on that molecule. Since there is no energy barrier for the guest triplet exciton to transfers back to the host, the number of triplet exciton transfer from guest to host per host monomer per unit time can be written as $w_{gh}=k_D n_g f$, where k_D is the intrinsic Dexter energy transfer rate. On the other hand, the Dexter energy transfer from the host to the guest has an energy barrier, so the transfer rate is $w_{hg}=k_D n_g n_T e^{-\beta\Delta}$. β is the inverse of thermal energy $k_B T$. T is temperature. In case of detailed balance we have $w_{gh}=w_{hg}$, which gives the Boltzmann distribution

$f=n_T e^{-\beta\Delta}$. Under a constant generation rate G of host triplet exciton per host monomer due to intersystem crossing from the host singlet exciton, the rate equations are

$$\dot{n}_T = -k_D e^{-\beta\Delta} n_g n_T + k_D n_g f - k_T n_T + G, \quad (1)$$

$$\dot{f} n_g = k_D e^{-\beta\Delta} n_g n_T - k_D n_g f - k_g f n_g. \quad (2)$$

Here k_T and k_g are the inverse lifetimes of the host and guest triplet excitons, respectively. The nonlinear decay like triplet-triplet annihilation is not included here because our system is under weak CW pumping. Indeed, the PA signals are always proportional to the pumping intensity in all measurements. For any initially formed host triplet exciton, eventually there are two possibilities for its final decay: either through its own direct decay to the ground state or through the decay of the guest triplet state. By definition the latter belongs to the Dexter energy transfer of the blend system and it is the fraction of the decay which can be detected by the slow component in the PL which shows up in the quadrature phase. The Dexter fraction z is expressed as $z = \frac{k_D n_g f}{k_T n_T}$. The steady-state solution of Eq. (2) gives

$$z = \frac{k_g n_g}{k_T} \frac{k_D n_g e^{-\beta\Delta}}{k_D n_g + k_g n_g}. \quad (3)$$

In PFO/Ir(mppy)₃ blend, the Dexter transfer rate $k_D n_g$ is at most one order of magnitude higher than the direct decay rate k_T of the host triplet exciton as shown in Fig. 3(a). Since k_T is about 10 s⁻¹ at 100 K, $k_D n_g$ is at most 100 s⁻¹. On the other hand, the guest decay rate k_g is as large as 106 s⁻¹. Therefore, for $n_g=0.1$ (10% doping), we always have $k_g n_g \gg k_D n_g$ in the denominator. As a result the Dexter transfer fraction z is simplified to

$$z = \frac{k_D n_g}{k_T} e^{-\beta\Delta}. \quad (4)$$

This form has transparent interpretations. The prefactor describes the competition between direct decay (k_T) and Dexter energy transfer ($k_D n_g$). Because of the energy barrier for Dexter transfer, the Boltzmann factor is also present. The result suggests that even without energy confinement some fraction of Dexter energy transfer is still possible if the host decay is very slow and the Dexter transfer is very fast. Our measurement can be used to give an estimate for the energy barrier Δ as below. As discussed above $\frac{k_D n_g}{k_T}$ is estimated to be about 10. The strength of the quadrature phase signal suggests that z is about 10⁻² at 100 K. Equation (4) then gives $\Delta \approx 0.07$ eV. In other words, while triplet exciton confinement is not necessary for Dexter transfer, the triplet energy for the green Ir can only be slightly larger than the host triplet exciton. Since the Ir(mppy)₃ triplet exciton energy is 2.38 eV from its phosphorescence, the host triplet exciton energy is estimated to at least 2.3 eV. This implies that a previous extremely-low-temperature optical measurement of the PFO triplet exciton energy of 2.1 eV is about 0.2 eV too low.²⁹ However, a room-temperature thermal measurement gives a quite consistent value of 2.3 eV.³⁰ Equation (4) implies that the Dexter transfer fraction decreases with tem-

perature exponentially with a fixed Δ . In Fig. 4(c) it does decrease as the temperature drops from 150 K to 24 K, supporting the assumption that energy is required in order to make the transfer. The decrease is, however, weaker than what Eq. (4) would predict. The weak temperature dependence might result from the random distribution of both the host and guest triplet energies due to morphological disorder.³¹ Because of the small barrier, it is likely that there is some overlap between the host triplet and the low-energy tail of the guest triplet. Such an overlap will make the temperature dependence weaker. Moreover, the value of Δ itself could be temperature dependent since the mean energies of the host and guest are expected to be different functions of temperature.

Let us then consider the situation that the guest triplet exciton energy is lower than the host by Δ , presumably for the case of the red Ir complexes. The rate equations become

$$\dot{n}_T = k_D e^{-\beta\Delta} n_g f - k_D n_g n_T - k_T n_T + G, \quad (5)$$

$$\dot{n}_g = -k_D e^{-\beta\Delta} n_g f + k_D n_g n_T - k_g f n_g. \quad (6)$$

The Dexter transfer fraction z is defined as before. The steady-state solution for Eq. (6) gives

$$z = \frac{k_D n_g}{k_T} \frac{1}{1 + \frac{k_D}{k_g} e^{-\beta\Delta}}. \quad (7)$$

It now becomes clear that even with a favorable energy and high doping of $n_g \sim 0.1$, significant Dexter transfer occurs only when the intrinsic Dexter transfer rate k_D over-

whelms the direct decay of the host triplet exciton. The absence of Dexter transfer for red Ir complexes suggests that $k_D n_g$ is smaller than 10^{-3} s^{-1} at low temperature. This implies that Dexter transfer depends sensitively on the particular molecular structures and aggregations. Even with the right energy, unfavorable structure or blend morphology could make the transition matrix element practically zero.

VII. CONCLUSION

In conclusion, PA and quadrature-phase channel PL have been employed to detect the Dexter energy transfer from polymer host to Ir guest in the polyfluorene blend systems. We observed Dexter energy transfer for green Ir(mppy)₃ but not for red DFIr and red BtpIr guests. The film morphology is found to be important for the existence of Dexter energy transfer. A fast Ir(mppy)₃ triplet exciton lifetime is responsible for Dexter energy transfer without triplet confinement. Based on this result it is possibility to utilize Ir complexes to harvest triplet excitons even without carrier trapping or triplet exciton confinement. In particular, a polymer host doped by blue phosphor with impossible triplet confinement could still be used for efficient blue PhPLEDX's if the lifetime of phosphor is fast enough.

ACKNOWLEDGMENTS

This work was supported by the National Science Council and the Excellence Project of the Ministry of Education of the Republic of China. The authors also thank RiTEK Corporation for supplying ITO substrates.

*Corresponding author. Electronic address: meng@mail.nctu.edu.tw

¹J. S. Wilson, A. S. Dhoot, A. J. A. B. Seeley, M. S. Khan, A. Köhler, and R. H. Friend, *Nature (London)* **413**, 828 (2001).

²M. Wohlgenannt, K. Tandon, S. Mazumdar, S. Ramasesha, and Z. V. Vardeny, *Nature (London)* **409**, 494 (2001).

³L. C. Lin, H. F. Meng, J. T. Shy, S. F. Horng, L. S. Yu, C. H. Chen, H. H. Liaw, C. C. Huang, K. Y. Peng, and S. A. Chen, *Phys. Rev. Lett.* **90**, 036601 (2003).

⁴H. H. Liao, H. F. Meng, S. F. Horng, J. T. Shy, K. Chen, and C. S. Hsu, *Phys. Rev. B* **72**, 113203 (2005).

⁵M. K. Lee, M. Segal, Z. G. Soos, J. Shinar, and M. A. Baldo, *Phys. Rev. Lett.* **94**, 137403 (2005).

⁶M. A. Baldo, D. F. O'Brien, M. E. Thompson, and S. R. Forrest, *Phys. Rev. B* **60**, 14422 (1999).

⁷M. A. Baldo, D. F. O'Brien, Y. You, A. Shoustikov, S. Sibley, M. E. Thompson, and S. R. Forrest, *Nature (London)* **395**, 151 (1998).

⁸M. A. Baldo, M. E. Thompson, and S. R. Forrest, *Nature (London)* **403**, 750 (2000).

⁹C. Adachi, M. A. Baldo, M. E. Thompson, and S. R. Forrest, *J. Appl. Phys.* **90**, 5048 (2001).

¹⁰X. Gong, J. C. Ostrowski, G. C. Bazan, D. Moses, and A. J. Heeger, *Appl. Phys. Lett.* **81**, 3711 (2002).

¹¹X. H. Yang and D. Neher, *Appl. Phys. Lett.* **84**, 2476 (2004).

¹²S. A. Choulis, V. E. Choong, M. K. Mathai, and F. So, *Appl.*

Phys. Lett. **87**, 113503 (2005).

¹³V. Cleave, G. Yahioglu, P. Le Barny, R. H. Friend, and N. Tessler, *Adv. Mater. (Weinheim, Ger.)* **11**, 285 (1999).

¹⁴M. A. Baldo, S. Lamansky, P. E. Burrows, M. E. Thompson, and S. R. Forrest, *Appl. Phys. Lett.* **75**, 4 (1999).

¹⁵X. Gong, J. C. Ostrowski, D. Moses, G. C. Bazan, and A. J. Heeger, *Adv. Funct. Mater.* **13**, 439 (2003).

¹⁶X. Gong, J. C. Ostrowski, D. Moses, G. C. Bazan, and A. J. Heeger, *J. Polym. Sci., Part B: Polym. Phys.* **41**, 2691 (2003).

¹⁷M. A. Baldo and S. R. Forrest, *Phys. Rev. B* **62**, 10958 (2000).

¹⁸I. H. Campbell, D. L. Smith, S. Tretiak, R. L. Martin, C. J. Neef, and J. P. Ferraris, *Phys. Rev. B* **65**, 085210 (2002).

¹⁹P. A. Lane, L. C. Palilis, D. F. O'Brien, C. Giebeler, A. J. Cadby, D. G. Lidzey, A. J. Campbell, W. Blau, and D. D. C. Bradley, *Phys. Rev. B* **63**, 235206 (2001).

²⁰Y. Y. Noh, C. L. Lee, J. J. Kim, and K. Yase, *J. Chem. Phys.* **118**, 2853 (2003).

²¹M. Wohlgenannt and Z. V. Vardeny, *Synth. Met.* **125**, 55 (2002).

²²A. S. Dhoot and N. C. Greenham, *Adv. Mater. (Weinheim, Ger.)* **14**, 1834 (2002).

²³F. C. Chen, G. He, and Y. Yang, *Appl. Phys. Lett.* **82**, 1006 (2003).

²⁴X. Gong, W. Ma, J. C. Ostrowski, G. C. Bazan, D. Moses, and A. J. Heeger, *Adv. Mater. (Weinheim, Ger.)* **16**, 615 (2004).

²⁵C. Adachi, M. A. Baldo, and S. R. Forrest, S. Lamansky, M. E.

- Thompson, and R. C. Kwong, *Appl. Phys. Lett.* **78**, 1622 (2001).
- ²⁶C. Adachi, R. C. Kwong, P. Djurovich, V. Adamovich, M. A. Baldo, M. E. Thompson, and S. R. Forrest, *Appl. Phys. Lett.* **79**, 2082 (2001).
- ²⁷Y. Sun, N. C. Giebink, H. Kanno, B. Ma, M. E. Thompson, and S. R. Forrest, *Nature (London)* **440**, 908 (2006).
- ²⁸S. R. Tseng, S. C. Lin, H. F. Meng, H. H. Liao, C. H. Yeh, H. C. Lai, S. F. Horng, and C. S. Hsu, *Appl. Phys. Lett.* **88**, 163501 (2006).
- ²⁹C. Rothe and A. P. Monkman, *Phys. Rev. B* **68**, 075208 (2003).
- ³⁰A. P. Monkman, H. D. Burrows, L. J. Hartwell, L. E. Horsburgh, I. Hamblett, and S. Navaratnam, *Phys. Rev. Lett.* **86**, 1358 (2001).
- ³¹V. I. Arkhipov, P. Heremans, E. V. Emelianova, and H. Bassler, *Phys. Rev. B* **71**, 045214 (2005).